OTC 25531

Post-simulations of Ice Basin Tests of a Moored Structure in Broken Ice – Challenges and Solutions

Basile Bonnemaire, Xiang Tan, Nicolas Serré, Arnt Fredriksen, Multiconsult AS; Ivan Metrikin and Arne Gürtner, Statoil ASA

This paper was prepared for presentation at the Arctic Technology Conference held in Copenhagen, Denmark, 23-25 March 2015.

Abstract

Interaction between a moored structure and drifting broken ice is a complex process. To document the expected structure response, ice basin tests of the interaction are common practice. The outcomes of ice basin tests need to be carefully analyzed before extrapolation to expected full-scale target responses. The preferred strategy is to use numerical simulations to correct the measurements. The numerical model needs to be qualified by successful post-simulations of the achieved ice basin interactions.

Post-simulations of interactions between drifting broken ice and a moored floating structure are of high complexity. The response of both the structure and the ice field needs to be replicated. This requires a good modeling of the ice field properties that matter (such as the floe size distributions and concentrations) and the boundary conditions affecting the interactions (such as the effect of the ice basin walls).

Statoil's SIBIS numerical model is used to post-simulate ice basin tests of the moored Cat-I drillship. The present paper discusses the challenges with such post-simulations and presents the philosophy chosen for achieving successful post-simulations.

Background

There is a limited experience with design and operation of moored structures in ice infested waters. Per today, the screening, feasibility or detailed design phases of such concept rely greatly on ice basin tests. This is inline with ISO 19906 (2010) normative requirements which states: "Appropriately scaled physical models and mathematical models may also be used to determine the response of structures to ice actions, in combination with current, wind and wave actions".

The outcome of ice basin tests has to be interpreted and corrected to be exploited in the design process. Different correction methods can be applied, and the use of empirical formulations is a common practice (see e.g. Tatinclaux, 1988). The interaction between a moored structure and drifting ice is a complex process, as changes in the action will affect the structure response and vice-versa. It can be challenging to only use empirical formulations to correct the measurements due to the complex interdependency between the ice action and the structure response. The preferred strategy to correct ice basin measurements is thus to combine ice basin tests with numerical modeling (see also Jensen et al., 2011, Bonnemaire et al., 2014):

1. Simulate numerically the ice basin tests, under achieved conditions,
2. Compare measurements and simulation outcome and qualify the numerical model for the considered interactions,
3. Use the qualified numerical model to simulate the response of the structure to the relevant ice interactions, under target conditions.

This methodology results in a correction of the ice basin outcome for the effect of all deviations in the achieved conditions under testing. In addition, the numerical model is qualified and can be used further for simulating additional similar interactions.

This procedure applied to moored floating structures in drifting ice is presented and discussed in for instance Jensen et al. (2011) and Bonnemaire et al. (2014). These studies focused on the interaction with intact level ice and ridges. The present paper discusses challenges and solutions in the application of the procedure for the interaction between a moored structure and drifting broken ice. Focus is put in particular on item 1 and 2, the post-simulation of ice basin tests. For an example on item 3 see Metrikin et al., 2015.

Challenges with post-simulations of broken ice interactions

Challenging aspects of ice basin tests of a moored structure in broken ice

Ice basin testing provides the best way to physically model the complex interaction between a moored floating structure and drifting sea ice. Apart from time consumption, ice basin tests are challenging with regards to the scaling of the interaction between a moored structure and drifting broken sea ice:

- Deviations and distortions: Model tests suffer from deviation and distortion of the target ice properties due to scaling effects (for instance distortion in the ratio crushing versus flexural strength). The achieved material and mechanical properties of model ice will not exactly be the target ones.
- Different driving forces: All the driving forces of drifting sea ice cannot be replicated in an ice basin, and usually the ice is stationary in the basin, and the structure is moved into the ice field.
- Boundary conditions: Ice basins are of limited size. Due to the challenge of scaling sea ice at a high scaling ratio, the scale is often kept as low as possible, and structure models are kept as large as possible. This increases the boundary effect challenges. Ice basin walls result in significant confinement effects on the broken ice field that affect the interaction on the structure. Interactions inside the ice field need to be well replicated (ice-ice friction, interlocking, failure of the ice floes…).
- Broken ice field properties: An additional challenge for ice basin tests in broken ice is to replicate the properties of the broken ice field (see example of ice basin broken ice field in Figure 1). The achieved floe size distribution and concentration will affect the interaction on the structure. This is in particular important at high concentrations (80% and up) where the ice actions are known to depend greatly on the concentration (Wright, 2000).
- Stochastic interaction process: Interactions with broken ice are often of high stochastic character:
    - The bearing capacity of the broken ice cover depends on the distribution and shapes of a large amount of ice pieces. The importance of these discrete particulars increases with the floe sizes. A small variation may lead to different response of the ice cover (e.g rotation of an ice floe instead of rupture) which in return will lead to a different action on the structure.
    - The action of broken ice on the vessel will vary through the penetration inside the ice cover depending on the local configuration of ice floes interacting with the structure. This may lead to varying ice action levels. The limited length of an ice basin limits in addition the interaction length.
    - These characteristics are challenging with regards to both repeatability of a given interaction, and estimation of statistical parameters of a response time series (such as expected extremes).

Figure 1 Examples of achieved broken ice field replica

Challenging aspects of post-simulations of interactions between a moored structure and broken drifting ice

Post-simulations aim at replicating the achieved interaction in the ice basin and comparing the simulated response and the measured one. Examples of successful post-simulations of a moored structure interacting with intact level ice and ridges are presented in Jensen et al. (2011) and Bonnemaire et al. (2014). Post-simulations of the response of a moored structure in broken ice are more challenging, and require:

- A numerical model able to simulate the interaction: The numerical engine should be able to model the following effects:
    - The dynamic response of the structure in all degrees of freedom. Examples are roll and pitch affecting the waterline and associated local ice-structure interaction, or the structure yaw affecting the relative ice drift direction on the structure and the structure effects on the ice field.
    - Ice field response around the structure and in the whole basin. This includes compaction, interlocking, formation of accumulations, rupture of ice floes…
    - Interaction at the interfaces (ice-structure and ice-basin walls). This includes the ice breaking processes, the friction effects, and the ice transport effects.
- A numerical replica of the achieved conditions under the interaction. A model of the interaction needs to be prepared in the numerical environment. This requires a good monitoring of the achieved conditions. Particular to interactions

with broken ice fields, is the replica of the macro properties of the ice field: floe size distribution, achieved concentration and local variations in the ice basin.

- Simulated responses that can be compared with measurements. An interaction between a moored structure and drifting broken ice involves the response of a large number of bodies. Full replica is not possible, and some deviations cannot be avoided. Due to the stochastic character of the interaction (see previous section), measured and simulated responses are then comparable with regards to trends, load levels and dependencies on the structure response or boundary effects. The stochastic nature of the interaction and the limited interaction lengths limits the possibility for advanced statistical comparisons.

Examples from successful post-simulations of a moored drillship in drifting broken ice

A drillship for operations in areas where ice may be present was designed by Inocean and Statoil. The Cat-I drillship was tested at the HSVA basin in the autumn 2013. Statoil's numerical model SIBIS was used to post-simulate ice basin tests of interactions between the moored Cat-I and drifting broken ice.

Figure 2 Ice basin tests of the moored Cat-I in drifting broken ice at HSVA. The vessel has an open-water bow and an icebreaking stern

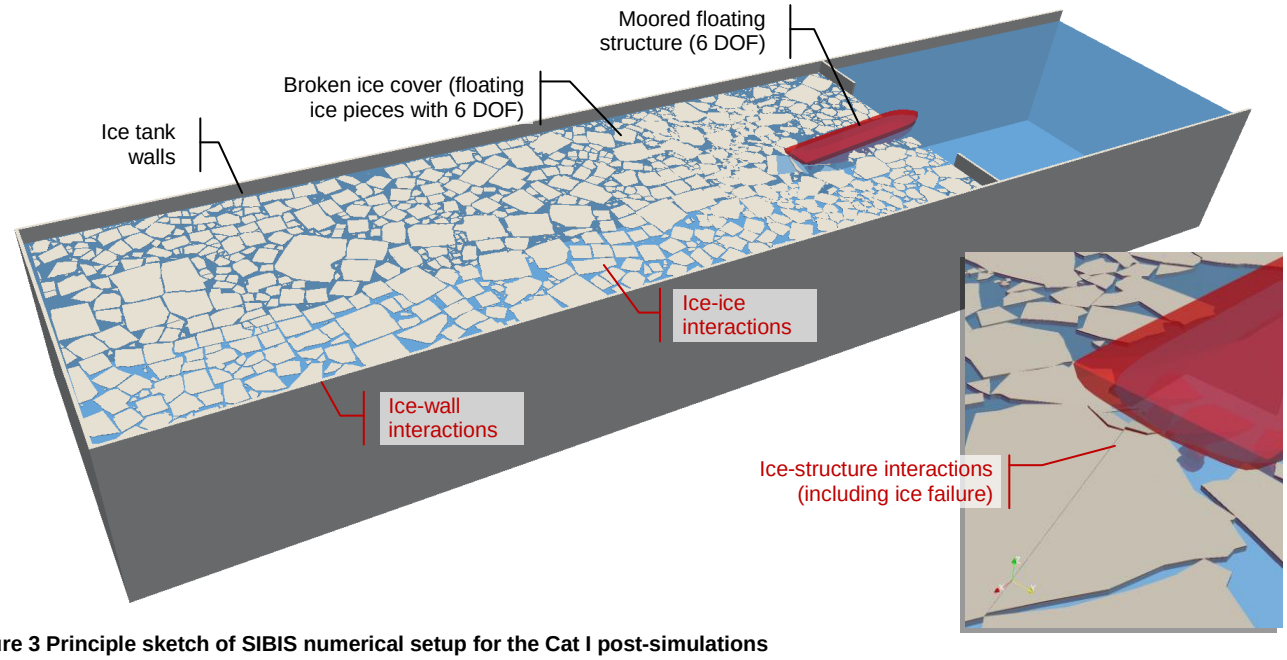

Figure 3 Principle sketch of SIBIS numerical setup for the Cat I post-simulations

Numerical set-up with the SIBIS engineering tool

The SIBIS model allows the simulation in the time domain of the response of stationary floating structure in drifting broken ice fields using the non-smooth discrete element approach. The SIBIS engineering tool has been developed jointly by Multiconsult and Statoil to address the challenges that the engineer is facing when for instance analysing ice basin tests through post-simulations..

Figure 3 presents a principle sketch of the numerical setup of the post-simulations:

- The Cat-I structure is moored to a carriage moving forward along the basin. The floating structure responds in 6 DOF to buoyancy, drag, mooring and ice forces.
- The ice cover is composed of ice floes responding in 6 DOF to accurate hydrostatic forces, skin and form drag forces, and the contact forces from other ice floes or structures. The ice floes can break in bending or splitting against the modelled structure. The broken ice field concentration and floe size distribution is similar to the ice basin ones.
- The ice basin is modelled with its wall confining the ice cover

A total of eight interactions performed in the ice basin were modelled numerically. This included ice covers of two different significant floe sizes, two ice thicknesses, and concentrations in the range 70 to 90 %.

Modelling of the achieved broken ice cover

The ice interaction and structure response depends on the broken ice macro properties (floe size, concentration) and the local variations (in concentration and floe size). Important parameters to replicate are:

- The total concentration: this controls the amount of ice mass in the ice field, and the available compliance in the ice cover.
- The floe size distribution: the relative amount of large floes and small floes will affect the ice cover response (such as rafting versus rubble accumulation under confinement).

The shape of the ice floes can also be replicated as it will affect to a certain extend how the floes interact (such as interlocking vs. sliding).

For the post-simulations of the HSVA ice basin tests, a numerical model of the achieved ice cover was built. HSVA prepared a bird view of the full ice field as before the interaction start and provided the achieved floes size distribution and concentration (see Figure 4a, c). The ice field picture is converted to a vector based format and a numerical field of 3D ice floes similar to the achieved one is prepared (see Figure 4b). The achieved numerical ice floe size distribution is compared with the ice basin distribution. This procedure ensures the production of ice fields that have similar concentration, floe size distribution, and ice floe shape.

Note that a good numerical replica of the ice field does not ensure that the structure will experience equal ice interactions (in the basin and in the numerical simulations). The ice field may be slightly perturbed after the picture is taken in the ice basin, and the ice field will be disturbed under the effect of the interaction. The vectorization process is neither fully accurate, and some discrepancies cannot be avoided.

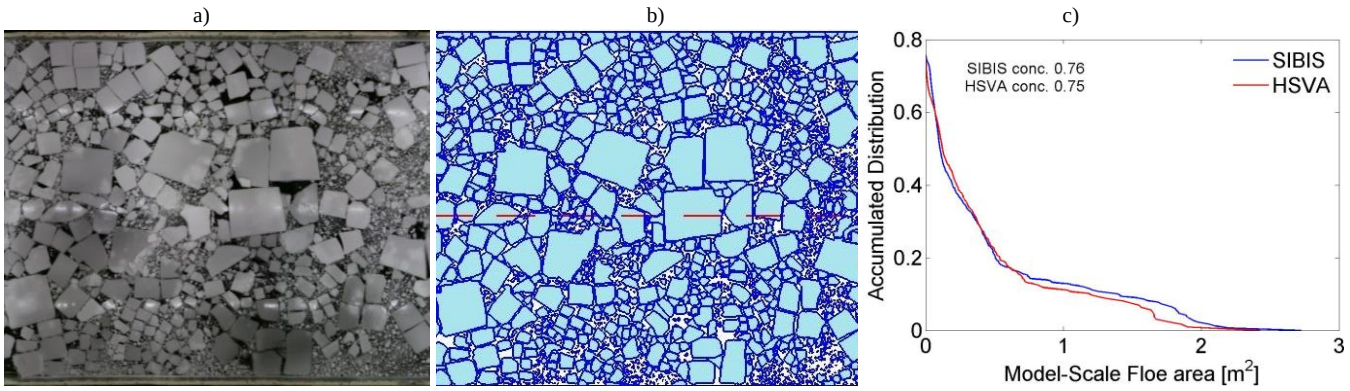

Figure 4 a) example of ice field picture from HSVA, b) corresponding ice field input to SIBIS, c) Comparison of floe size distribution and concentration.

Examples of post-simulation outcomes

The simulations outcomes were compared with the available observations. Focus was put on the major processes that govern the global response level:

- Response of the ice field: Mobilization of the ice field, confinement increase due to the boundary effects and interlocking effects were observed and compared (see example in Figure 5). The ice field response will depend on the relative importance of different effects: water drag effects, pressure and frictional effects from neighboring bodies, collapse of the field (due to local rupture of ice floes, rafting or rubbling effects). This will govern the global bearing capacity of the ice field.
- Ice failure mode and ice accumulation against the structure: The ice failure at the vessel interface limits the action from the ice field on the structure. The different failure modes (bending, splitting, crushing) will have different effects. The accumulation of ice upstream and around the structure will also affect the ice actions on the structure. It is thus important to replicate the in-plane and sub-surface ice transports effects.

- Response of the structure: The structure response in roll, pitch and heave affect the waterline and the ice interaction process at the ice-structure interface. The yaw response of the structure affects the exposed size of the structure and affects the ice field around the structure. In addition, the structure response (such as tilt) can be a design criteria.
- Mooring loads: The mooring load is governed by the structure response (mooring offset). Mooring load is a design criteria and should be replicated.

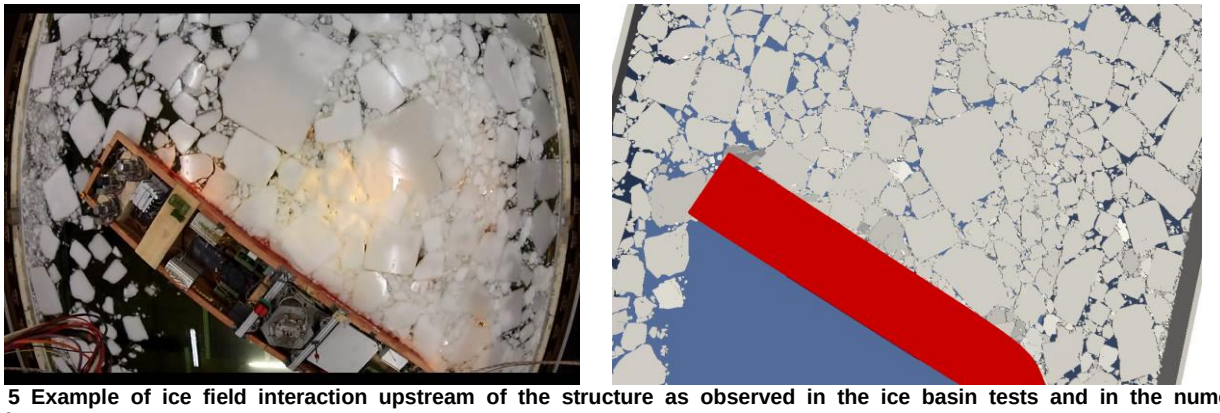

Figure 5 Example of ice field interaction upstream of the structure as observed in the ice basin tests and in the numerical simulations

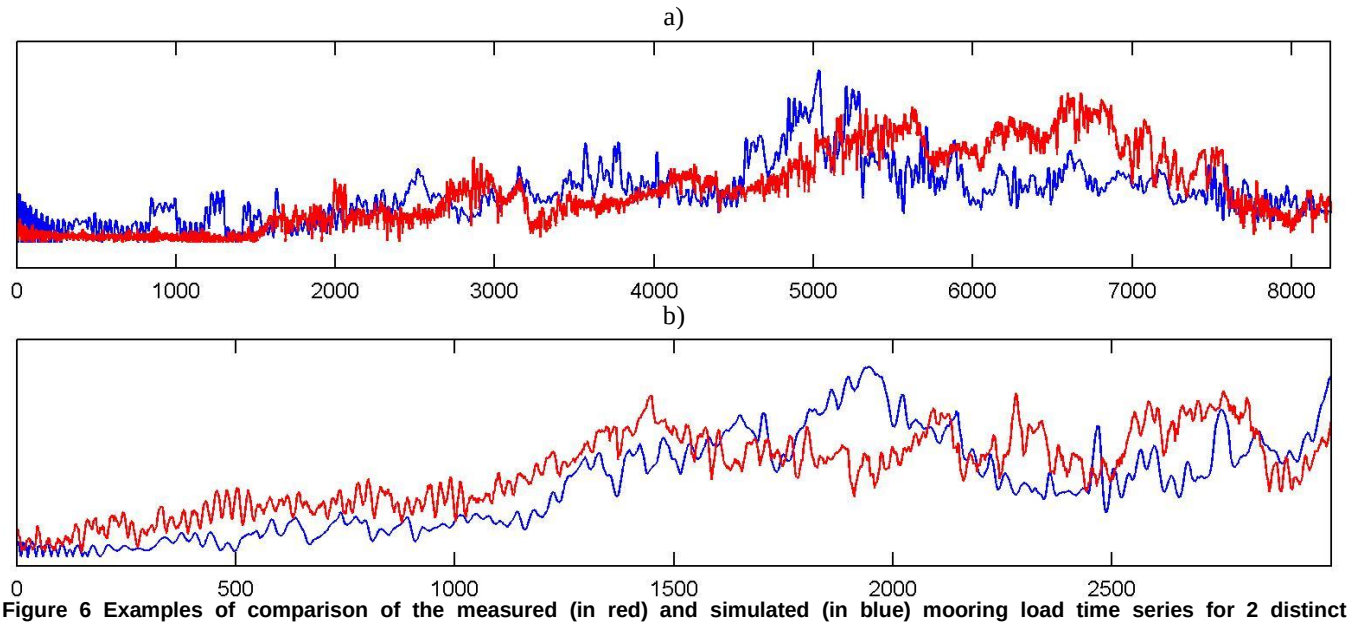

Figure 6 Examples of comparison of the measured (in red) and simulated (in blue) mooring load time series for 2 distinct interactions, a) 90 % concentration, large floes, b) 90 % concentration, small floes

Post-simulations are successful when the numerical simulations of these effects are similar to the observed ones. Figure 6 gives two examples of comparison of achieved and simulated mooring load levels.

- The load time series show that similar mooring load levels and trends are achieved along the ice basin.
- However, the time series can differ locally. Exact replica is not expected due to the nature of the interactions. The interactions with broken ice are highly stochastic, and a small perturbation at some point result into a different interaction.
- The interactions are short with few main oscillations. It is challenging to compare the extreme values as several oscillations (longer interaction) may result in different extremes.

Summary and Conclusions

The outcomes of ice basin tests need to be carefully analyzed before extrapolation to expected full-scale target responses. The preferred strategy is to use numerical simulations to correct the measurements. One needs then a numerical model able to replicate the interaction achieved in the ice basin.

Post-simulations of interactions between drifting broken ice and a moored floating structure are of higher complexity than post-simulations in intact level ice or ridges. From the authors point of view, the engineer should not target at exactly replicating numerically such interaction, in particular as:

- A full measurement of the interaction scene is not available,
- The interaction is of high stochastic character, and a small perturbation will easily affect the chain of events

However, it is shown in this paper that by focusing on replicating chosen properties and processes that steer the interaction, one is able to replicate similar interactions presenting similar response levels. The SIBIS numerical model was successfully used to post-simulate ice basin tests of the moored Cat-I drillship.

Acknowledgements

The authors are grateful of the support, assistance and trust shown by Pavel Liferov (Statoil), Jørgen Jorde (Inocean) and the HSVA experts. The present work would not have been possible without the assistance and dedication of Trine Lundamo, Åse Ervik, Dmitry Sapelnikov and Arnor Jensen (Multiconsult).

References

Bonnemaire B., N. Serré, T. Lundamo, A. Fredriksen and A. Jensen, A. Gürtner and S. Teigen, 2014. Ice breaking and accumulation around a moored structure: ice basin tests and numerical simulations, OTC 24579, Arctic Technology Conference, Houston, Texas, USA, 12- February 2014

ISO/FDIS 19906, 2010. Petroleum and natural gas industries – Arctic offshore structures, ISO TC 67/SC 7. Final Draft International Standard, International Standardization organization, Geneva, Switzerland, 434p.

Jensen, A., B. Bonnemaire T. Lundamo, O. Ravndal (2011): Efficient combination of numerical simulations and ice basin testing in the design process of moored structures in ice. Offshore Technology Conference; Arctic Technology Conference, Houston, Texas, USA, 7–9 February 2011

Ivan Metrikin, Sigurd Henrik Teigen, Arne Gürtner, Eirik Strøm Uthaug, Dmitry Sapelnikov, Åse Ervik, Arnt Fredriksen, Trine Lundamo, Basile Bonnemaire (2015): Experimental and Numerical Investigations of a Ship-Shaped Turret-Moored Floating Structure in Intact and Managed Sea Ice Conditions; Arctic Technology Conference, Copenhagen, Denmark, 23-25 March 2015

Tatinclaux, J.P., 1988: Ship model testing in level ice – An overview. CREEL report 88-15

Wright, B., 2000: Full Scale Experience with Kulluk Stationkeeping Operations in Pack Ice. PERD/CHC Report 25-44

OTC 22572

The Seasonal Cycle of Sea Ice Thickness on the North East Greenland Shelf

E. Hansen, Multiconsult/Norwegian Polar Institute; S. Gerland, G. Spreen, Norwegian Polar Institute; and K. Høyland, Norwegian University of Science and Technology (NTNU)

Abstract

The seasonal cycle of sea ice thickness on the North East Greenland shelf as derived from 22 years of direct observations with upward looking sonars is quantified. The seasonal cycle of the mean and modal thickness is presented, both as absolute numbers and as anomalies from the annual mean. The average seasonal amplitude for the whole observational period (1990-2011) is 0.5 m for the modal thickness, and 1.12 m for the mean ice thickness. The mean cycle was also calculated for two distinct periods with respect to the age and thickness of the ice in the region; 1990-2000 and 2001-2011**.** Between these two periods, the average seasonal amplitude in modal thickness was reduced by 0.2 m. For the mean ice thickness, the corresponding reduction was 0.3 m. In addition the seasonal cycles were shifted down. The results presented here are directly applicable for industry planning activities on the North East Greenland shelf, and are particularly useful for oil companies holding licenses in the Kanumas area. The seasonal and interannual variability of sea ice thickness is large in this region. Any plan for field development or operations in the region must take this variability into account. This includes ice thickness observation campaigns (e.g. by airborne electromagnetic devices) set up to provide details about the design basis prior to field development, where it is imperative that the observations are interpreted on a background of variability. Along with previously published results on long term variability, the present results on the seasonal cycle provide such a background.

Introduction

The North East Greenland shelf, and particularly the Kanumas license region, is expected to hold significant amounts of hydrocarbon resources. It is therefore a region of considerable interest for energy companies with Arctic aspirations. In terms of sea ice the region is particularly challenging, with multiyear sea ice being steadily delivered from the Arctic Ocean trough Fram Strait. This continouous delivery of sea ice represents the southern limb of the Transpolar Drift. The Kanumas region is therefore featuring extensive and very thick sea ice. At its northern borders, the thickness of old level ice frequently exceeds 3.0 m, ranging up to 3.6 m [1]. During winter, the fraction of ice thicker than 5 m (pressure ridges) may peak well above 25% [1]. The deepest keel draft observed is 35 m, with estimated 100-year return period drafts up to 41 m [2]. The mean keel draft is typically 7.3 m [3].

Arctic sea ice has become significantly thinner during the first decade of the 21st century [4], with concurrent changes in age composition towards more first-year ice (sea ice of not more than one winter growth) at the expense of old ice (sea ice that has survived at least one summer melt season) [5] [6]. The loss of the oldest ice types has been particularly extensive, implying that the age of the remaining old ice is reduced. Following record low old ice coverage in summer 2008, the total coverage of old ice increased again; by 2011 the level were again consistent with the downward trend during the early 2000s [6].

This general basinwide reduction in Arctic sea ice age and thickness is reflected in observations of ice age and thickness in Fram Strait, at the northern borders of the Kanumas region. Along with an increasingly younger ice cover in the region, the ice thickness was reduced by ~30% comparing 2007-2011 versus the 1990s [1]. During 2003-2012 the thickness of ice observed at the end of the melt season became 50% thinner [7]. There is also a significant reduction in the number and mean keel draft of pressure ridges [8]. This longterm thinning trend appears superimposed on variability on shorter timescales, both

interannual/decadal [9][10] and seasonal.

The seasonal cycle of Arctic sea ice thickness is not well quantified. This includes the ice found on the North East Greenland shelf. The continuous and concurrent work of thermodynamic and dynamic processes operating on the ice to change its thickness – with different effects in different segments of the range of ice thickneses – complicates both the understanding of the role of the processes and our ability to quantify their effects. The lack of observational data with sufficient temporal and spatial coverage and resolution further complicates this issue. As an example, we could mention that when scientists adjust their large scale ice thickness data sets to take seasonality into account, they normally rely on model data (e.g. [4]).

This paper quantifies the seasonal cycle of sea ice thickness on the North East Greenland shelf as derived from 22 years of direct observations with upward looking sonars. The seasonal cycle of the mean and modal thickness is presented, both as absolute numbers and as anomalies from the annual mean. The mean cycle is calculated for two distinct periods with respect to the age and thickness of the ice in the region.The results are directly applicable for industry planning activities on the North East Greenland shelf, and are particularly useful for oil companies holding licenses in the Kanumas area. The seasonal and interannual variability of sea ice thickness is large in this region. Any plan for field development or operations in the region must take this variability into account. This includes ice thickness observation campaigns (e.g. by airborne electromagnetic devices) set up to provide details about the design basis prior to field development, where it is imperative that the snap shot observations are interpreted on a background of variability. Along with previously published results on long term variability [1][9][11][10], the present data on the seasonal cycle provide such a background.

Data and methods

The principles of upward looking sonars used to observe ice draft are illustrated in Figure 1. The instruments record the return travel time of emitted sound pulses. Based on sound speed derived from temperature and salinity sensors beneath the sonar, the travel time is converted to range r (Figure 1). In addition temperature, pressure (P_{btm}), and instrument tilt (θ) are recorded. The sea level above the instrument is calculated as $\eta = (P_{btm}-P_{atm})/\rho g - \Delta D$. Here P_{atm} is the atmospheric pressure (taken from the nearest meteorology station or from reanalysis products). ΔD is the vertical distance between the pressure sensor and the acoustic transducer (range sensor), while g is the local acceleration due to gravity. The draft is then calculated as $d = \eta - r \cdot \cos(\theta)$.

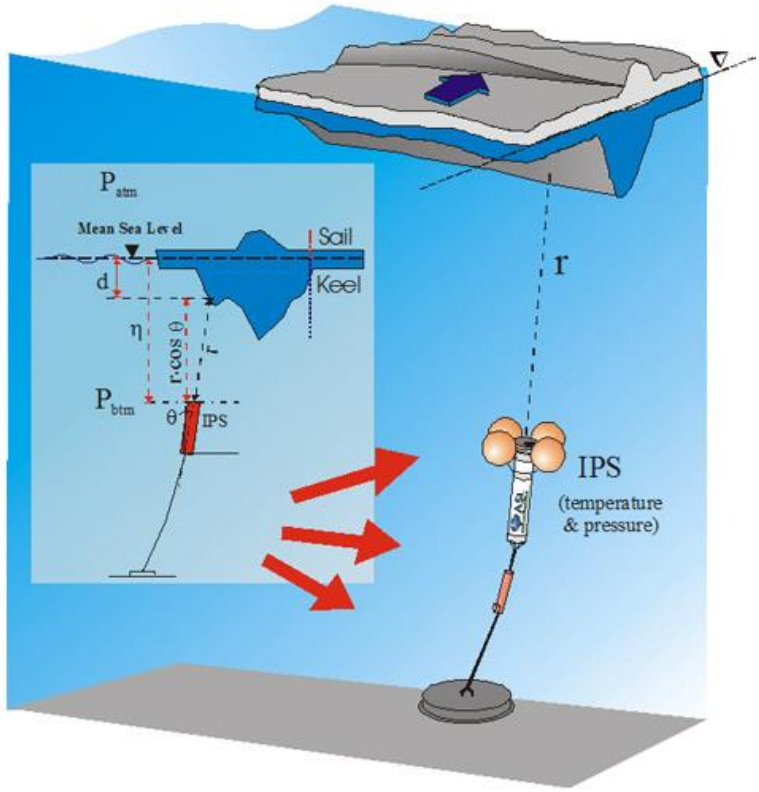

Figure 1 The principles of observing sea ice draft by upward looking sonars moored on the seabed. The instruments record the return travel time of emitted sound pulses, as well as temperature, pressure, and instrument tilt. The sea ice draft d is calculated as illustrated in the figure (illustration courtesy of ASL Environmental Sciences Inc.).

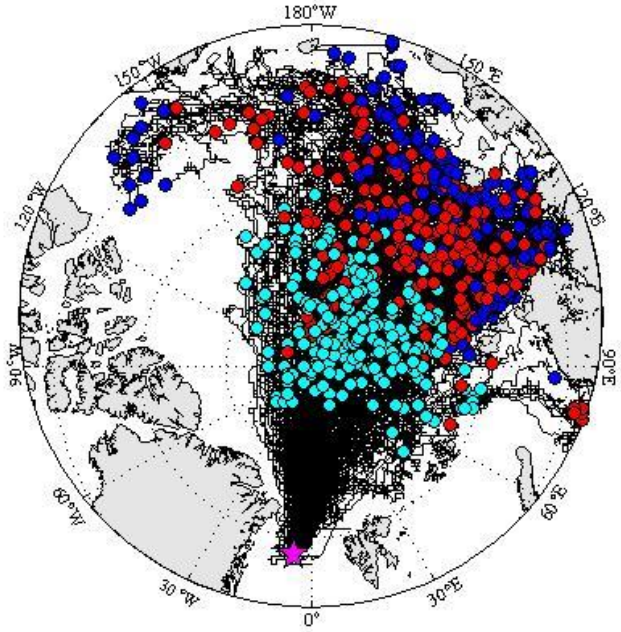

Figure 2 The origin of the observed sea ice, in terms of its drift trajectories (black lines) and position 1 year (cyan bullets), 2 years (red bullets) and 3 years (blue bullets) prior to its export through Fram Strait. The position of the observation site at 79 N 5 W in Fram Strait is indicated (magenta star), from wich all back trajectories are calculated.

The Norwegian Polar Institute has maintained an array of up to four moored upward looking sonars (ULS, CMR ES300 instruments) across the Transpolar Drift where it exits the Arctic Ocean in Fram Strait since 1990 (Figure 2, and references[1] [11]). Since 2006 the observations have been made by ice profiling sonars (IPS, ASL Environmental Sciences IPS4 and IPS5 instruments). In this study we have used instruments positioned at 79° N 5° W. The location is illustrated in Figure 2. All data were processed by ALS Environmental Sciences according to their standard processing routines [12]. Further details about the processing and data management are found in [1].

The sonars measure ice draft. But as most other studies refer to ice thickness, we prefer to present our numbers as thicknesses. Following earlier work on the data set [1][9][12][13], we use a constant ratio between thickness and draft of 1.136 [14] to carry out the conversion.

All IPS instruments sampled with an interval of 2 s, which resolved all thickness features well and ensured smooth ice thickness distributions. The ULSes sampled with a four minute sampling interval (except for the 1990-1991 deployment which used a sampling interval of eight minutes). The ice thickness observations were converted into monthly distributions of 0.1 m bin size. The smooth character of the IPS distributions indicates that this is within the accuracy of the observations. In the following, all numbers are therefore listed with 0.1 m precision. Noise introduced by the long sampling intervals during the 90s was removed by using a kernel density estimator when constructing the distributions (Gaussian kernel, bandwidth 0.1 m). The resulting smooth distributions enabled us to identify distinct modes while keeping the statistical properties of the original time series.

The results presented here are based on ice thickness distributions which are time referenced. As the sampling interval is fixed and the ice drift over the sonars is varying with time, the statistics could potentially change with changing drift velocities for instruments with long sampling intervals. The longer sampling intervals could also potentially lead to underrepresentation of the thick ice, as the ridge keels could be missed. We simulated this effect by subsampling the post 2005 IPS data, which are sampled with an interval of 2 seconds. The subsampling showed that the thickness distribution is well resolved on a monthly basis, even with a sampling interval as long as 8 minutes. Also the tail is resolved. We also found that summary statistics like the mean, mode, median and interquartile range did not change with increasing sampling interval up to 8 minutes. We take this as a confirmation that the statistics based on monthly distributions are robust.

Three year backward drift trajectories were calculated for each month of the 1990-2011 period, in order to have a control on the origin and pathway across the Arctic of the ice observed in Fram Strait. The calculation is based on available Arctic wide sea ice motion vector data sets. For the 1990-2006 period we used the Polar Pathfinder Daily 25 km EASE-Grid sea ice motion vectors data set available at the National Snow and Ice Data Center (NSIDC, [15]). The period 2007-2011 is not covered by this data set. To cover this period we used daily sea ice motion vectors derived from merged QuikSCAT, ASCAT

and SSM/I data, available on a grid resolution of 62.5 km from the Center for Satellite Exploitation and Research at the French Research Institute for Exploitation of the Sea (CERSAT Ifremer, [16]). The latter data set does not cover the summer months (June, July and August). In order to facilitate the calculation of three year drift trajectories, each summer gap was filled with the 1990-2006 mean summer velocity field derived from the corresponding Polar Pathfinder data set. The backtracking was performed from the position of the observation site in Fram Strait at 79° N 5° W, starting from the last day of each month. Stepping back day by day, the estimated position of the patch of ice was calculated until land, fast ice or open water was encountered.

Based on the ice thickness observations, monthly ice thickness distributions were established. The seasonal cycle of the modal thickness (the thickness of old level ice) was calculated by first identifying the mode in each monthly ice thickness distribution. Then all the modal thicknesses belonging to each calendar month were averaged, over each of the 12 calendar months. The seasonal cycle of the mean ice thickness was established in the same way. Since the seasonal cycle is superimposed on a thinning trend [1], we also calculated the seasonal cycle of the modal and mean thickness anomalies. For each monthly value we subtracted the annual mean, yielding the anomaly. The seasonal cycle of the anomaly was calculated by averaging the monthly anomaly for each calendar month. This parameter then conveys how the modal and mean thickness are varying around the annual mean for each year. In this way we are separating the true seasonal cycle, and have removed the effect of the downward trend in thickness [1].

All versions of the seasonal cycle were calculated for 1) the whole 1990-2011 period, 2) 1990-2000, and 3) 2001-2011. The two latter periods are distinct with respect to the age and thickness of the sea ice; the first period featured older and hence thicker ice than the last period.

Results

The source region of the sea ice is not an important issue if one is solely interested in the actual ice thickness values on the North East Greenland shelf. However, in understanding the thickness variability it is imperative that we separate the role of variability in advection from the role of variability in dynamic and thermodynamic processes. The source regions of sea ice observed in Fram Strait are indicated through the spread of three-year backward drift trajectories shown in Figure 2. The position of a patch of sea ice one, two, and three years prior to its export through Fram Strait is indicated in the same figure. During most of the 1990-2011 period the ice was found in the central Arctic Ocean (north of 85° N) one year before it was exported through Fram Strait. Two or three years prior to its export, most of the ice was located in or just north of the Laptev and East Siberian Seas. These seas are the dominant providers of sea ice to the Transpolar Drift and our monitoring site. The exceptions to this pattern are of episodic nature (for example the trajectories in Figure 2 originating in the Beaufort and Chukchi Seas, as well as the Kara Sea). This means that over the years we are comparing the thickness of ice of roughly the same origin, namely the Siberian shelf seas. Moreover, there is no pronounced seasonal cycle in sea of origin. This implies that the seasonal cycle in thickness presented here is largely due to the seasonality in thermodynamic and dynamic processs, and not due to seasonality in the advection pattern.

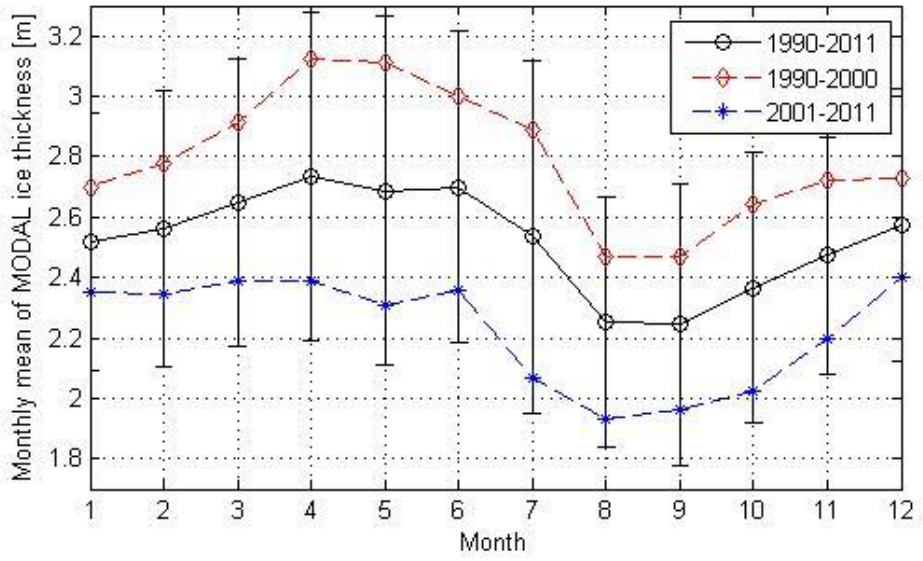

Figure 3 The seasonal cycle of the modal thickness (the thickness of old level ice). The average seasonal cycle for the whole 1990-2011 period (black) is shown with errors bars showing the standard deviation (+/-) of the monthly average. The cycles for the 1990-2000 (red) and 2001-2011 (blue) periods are shown without error bars.

Table 1 The average seasonal cycle of the modal and mean ice thickness during 1990-2011 (all numbers in meter)

	Jan	Feb	Mar	Apr	May	Jun	Jul	Aug	Sep	Oct	Nov	Dec
Modal thickness (1990-2011)	2.52	2.56	2.65	2.74	2.69	2.70	2.54	2.25	2.24	2.37	2.47	2.57
Mean thickness (1990-2011)	2.81	2.87	2.90	3.01	3.09	3.26	3.11	3.01	2.14	2.50	2.87	2.90

The average seasonal cycle in modal thickness (the thickness of old level ice) over the 1990-2011 period is shown in Figure 3 and listed in Table 1. On average, the minimum modal thickness is reached in August-September (~2.25 m). The maximum thickness is reached in April (2.74 m). This yields an average seasonal amplitude of 0.5 m, around an average modal thickness of 2.52 m over the year. This is the work of thermodynamical processes during freeze up and melt.Clearly the magnitude of thickness gain or loss during the seasons varies with the factors controlling the seasonal freeze up and melt. In addition to the thermodynamic factors, the age of the ice is a major factor in controlling the level of the thickness which the seasonality cycles around. Hence advection also plays a role in the sense that ice that is not exported to lower latitudes may survive the melt season to form older ice. The average seasonal cycle observed in Figure 3 is reflecting the work of the average thermodynamic factors and the prevailing age of the ice during this period.

The years 1990 to 2011 was a period of decreasing ice age and modal thickness in Fram Strait [1]. The effect on the seasonal cycle of modal thickness is illustrated in Figure 3, where the average seasonal cycle calculated for the 1990-2000 period is contrasted to the average seasonal cycle over the years 2001-2011. In the latter period the cycle is shifted down, and the amplitude is reduced. During the 1990s the average seasonal maximum modal thickness peaked to 3.13 m in April. During the 2000nds the corresponding number was reduced to 2.39 m. For the ice thickness minimum in August the value of 2.47 m during the 1990s was reduced to 1.93 m during the 2000nds. Hence the average seasonal amplitude was reduced from 0.66 m to 0.46 m between the two decades.

The average seasonal cycle of the mean ice thickness in Fram Strait over the 1990-2011 period is shown in Figure 4 and listed in Table 1. The monthly mean ice thickness is calculated as the aritmethic mean of all thickness observations during each month since the onset of the observations in 1990. Unlike the modal thickness, which is reflecting the thickness of old level ice and where the variability reflects variability in thermodynamic processes, the mean ice thickness is influenced by all available ice types. Moreover, variability in the mean ice thickness generally reflects variability in both thermodynamic and dynamic processes acting on the ice to change its thickness. Clearly the mean ice thickness it is not a summary statistic which is well suited to describe ice thickness change or to point to likely causes for the change. However, it is much used to describe the thickness of the ice cover in reports from large scale ice models or large scale ice thickness observations (remote sensing), or in reports based on ice thickness data sets where the temporal and spatial coverage does not allow more details than the mean thickness to be deduced. We therefore include the mean ice thickness in our analysis.

On average, during 1990-2011 the maximum seasonal mean ice thickness is reached in June, when it peaks to 3.26 m. The seasonal minimum is reached in September at 2.14 m. The average seasonal amplitude of mean ice thickness is therefore 1.12 m, around an annually averaged mean thickness of 2.87 m. In addition to the thermodynamic processes and ice age which controls the thickness of level ice, the mean ice thickness is also controlled by dynamic processes (rafting, ridging and rubble building). The mean ice thickness is dominated by dynamically deformed ice, due to the generally great thicknesses of this ice type. On average 66% of the mean ice thickness is due to deformed ice in this region [9]. However, it is not straightforward to separate between the role of dynamic and thermodynamic processes in controlling the seasonal thickness change.

The genereally decreasing ice age and ice thickness in Fram Strait [1] is reflected also in the seasonal cycle of the mean ice thickness. Again we contrast the average seasonal cycle over the years 1990-2000 to the cycle of the following decade of 2001-2011. We refer to the two periods as the 1990s and the 2000nds, respectively. The average seasonal cycle was somewhat shifted down during the period (Figure 4). But unlike the change in the seasonal cycle of the modal thickness, the change in mean ice thickness is less constant over the year. Hence the change has more character of a change in shape of the cycle, rather than a shift. During the 1990s the seasonal maximum mean ice thickness peaked to 3.63 m. During the 2000nds the corresponding number was reduced to 2.83 m. The average seasonal ice thickness minimum in September was 2.37 m during the 1990s, and 1.87 m during the 2000nds. Hence the average seasonal amplitude in mean ice thickness was reduced from 1.26 m during the 1990s, to 0.96 m during the 2000nds.

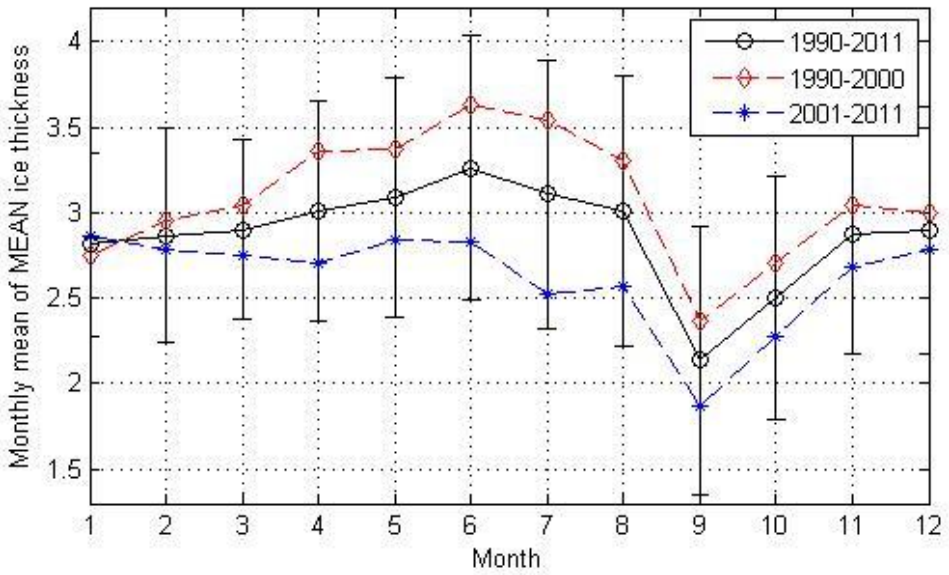

Figure 4 The seasonal cycle of the mean ice thickness. The average seasonal cycle for the whole 1990-2011 period (black) is shown with errors bars showing the standard deviation (+/-) of the monthly average. The cycles for the 1990-2000 (red) and 2001-2011 (blue) periods are shown without error bars.

Figure 3 and Figure 4 show how the absolute modal and mean ice thickness cycle over the year. However, these average seasonal cycles are calculated for periods which feature large variability in thickness on interannual to decadal time scales [1][9]. We are therefore interested in the seasonal cycle of the thickness anomaly, i.e., a quantification of how the thickness cycle around its mean value each year. This shows how the seasonal cycle is expected to behave under a given prevailing ice thickness.

The thickness anomaly was calculated for the modal and mean ice thickness. For each month of the time series, the mean value of the thickness (mode or mean) for all 12 months in the year that the month belongs to, was subtracted from the monthly value. This yields the thickness anomaly. Then all the thickness anomalies (for modal and mean ice thicknesses, respectively) belonging to each calendar month were averaged, over each of the 12 calendar months.

The result is shown in Figure 5. The seasonal amplitude of the modal thickness calculated through the modal thickness anomaly is roughly the same as the corresponding cycle calculated directly from the absolute values. One thing worth noting is that during the 1990s, the modal thickness anomaly at the end of winter/onset of melt was higher than the corresponding number during the 2000nds (the difference is 0.21 m). The modal thickness anomaly at the end of summer/onset of freeze is the same for the two periods. In short, this means that the old level ice was 0.21 m thicker (on average) at the onset of melt during the 1990s than during the 200nds, relative to the prevailing thickness during these periods. One may also observe that at the onset of freeze in September the rate of freeze up was higher during the 1990s than during the 2000nds. However, during October the situation reverses, and the freeze up rate is faster during the 2000nds than during the 1990s. This leads to higher modal thickness anomalies early in the winter during the 2000nds. Also, there is no pronounced peak in the winter maximum for the 2001-2011 period. During this period, there was a larger spread in the timing of maximum (month of occurence) than during the preceeding period [1]. The cause of this spread is not immediately obvious, but the age of the ice is a likely contributor. When the ice is younger and thinner, it is more exposed to variability in the thermodynamic boundary conditions. Hence, an occasional cold spell during winter is likely having a greater impact on the thickness when the ice is young and thin. With the age of the ice being consistently lower during the 2000nds, we could be seeing the effect of this mechanism.

For the mean ice thickness anomaly one may observe that the ice was thicker at its maximum in June during the 1990s than during the 2000nds. However, since this was the case also during the minimum in September, the seasonal amplitude of the mean ice thickness anomaly did not change much between the two decades. The main feature to note is that during the 2000nds the maximum thickness after winter and at the onset of melt and ridge disintegration was lower than during the preceeding period, and that the melt or ridge disintegration process appears to have taken place faster. One may also observe that during winter (Jan-March) the mean ice thickness anomaly was higher during the 2000nds. The underlying causes and mechanisms controlling these changes are subject to further work.

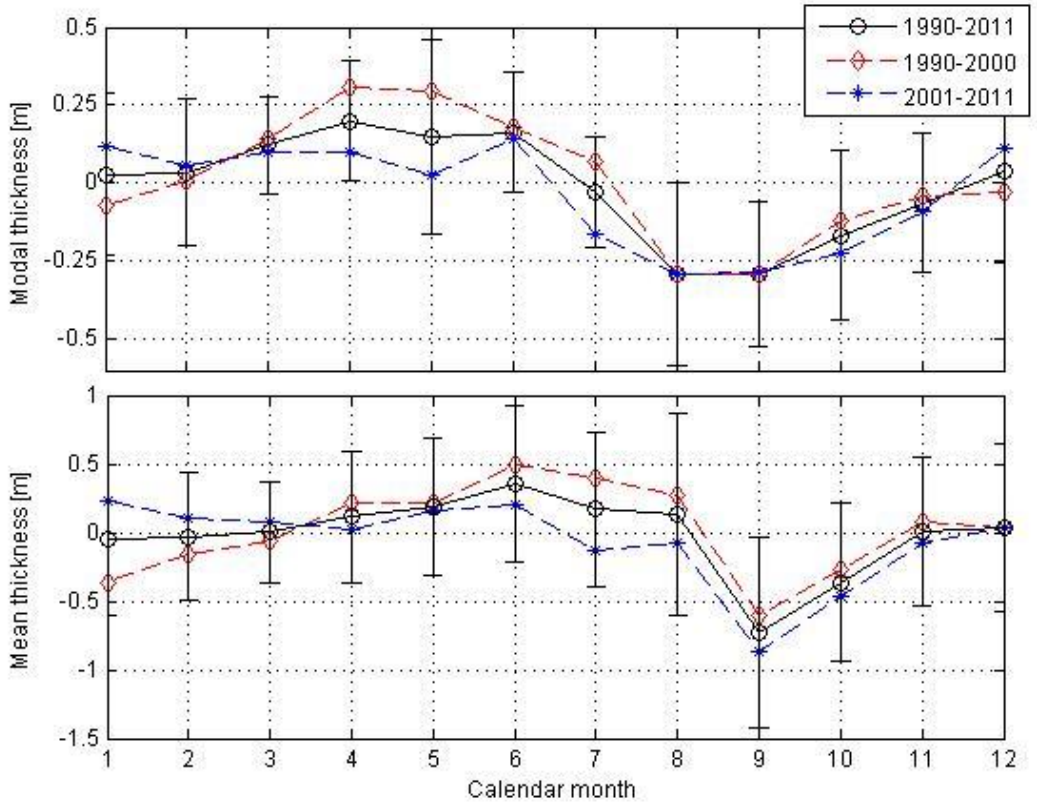

Figure 5 The average seasonal cycle of the ice thickness anomaly, i.e., the diffrence between the ice thickness (modal and mean) for each month and the average value each year. The anomaly of the modal thickness is shown in the upper panel, while the lower panel shows the corresponding cycle for the mean ice thickness.

Summary and conclusions

We have presented the average seasonal cycle of modal and mean ice thickness as derived from ice thickness observations by moored upward looking sonars in Framstrait (79° N °5 W). This location is at the northern boundary of the Kanumas license area. Hence, the significance of this paper lies in its presentation of the (hitherto unknown) seasonal cycle of ice thicknesses representative for the Kanumas license area. The most important addition to the technical knowledge base of the petroleum industry is the quantification of the range of thicknesses which may be expected, month by month over an average year. Another addition is the knowledge on the transition into different seasons, which is useful for planning of operations. The long time series also enables us to quantify variability. Not only in terms of a seasonal cycle, but also how this cycle is changing over time.

We have showed that the average (1990-2011) seasonal cycle of modal thickness in this region is spanning from a summer minimum of 2.25 m in August, to a winter maximum of 2.74 m in April. This means a seasonal amplitude in the modal thickness (i.e., the old ice level thickness) of 0.5 m. Following the generally decreasing age and thickness of the Arctic sea ice, this amplitude was reduced during the observational period. During the observational period the amplitude was reduced by 0.20 m.

We have also showed that the seasonal cycle of the mean ice thickness in this region is spanning from a summer minimum of 2.14 m in September, to a maximum following winter of 3.26 m in June. This is an average seasonal amplitude in the mean ice thickness of 1.12 m. This amplitude was also reduced during 1990-2011. Comparing the average amplitude during the 2000nds to that of the 1990s, a reduction of 0.3 m was observed.

Due to the steady inflow of sea ice from the Arctic Ocean, the seasonal and interannual variability of sea ice thickness is large in this region.Any plan for field development or operations in the region must take this variability into account, by planning with this variability in the background. Along with previously published results on long term variability, the present results on the seasonal cycle provide such a background.

References

[1] Hansen, E., S. Gerland, M. A. Granskog, O. Pavlova, A. H. H. Renner, J. Haapala, T. B. Løyning, and M. Tschudi (2013), Thinning of Arctic sea ice observed in Fram Strait: 1990-2011, J. Geophys. Res.,Vol. 118, doi:10.1002/jgrc.20393.

[2] Ekeberg, O-C., K. Høyland, and E. Hansen (2013), Extreme keel drafts in the Fram Strait 2006-2011, Proceedings of the 22nd International Conference on Port and Ocean Engineering under Arctic Conditions (POAC), June 9-13, 2013, Espoo, Finland.

[3] Ekeberg, O. C., Høyland, K., and E. Hansen (2014), Ice ridge keel geometry and shape derived from one year of upward looking sonar data in Fram Strait, Cold Regions Science and Technology, 109 (2015) 78-86, doi 10.1016/j.coldregions.2014.10.003.

[4] Kwok, R., and D. A. Rothrock (2009), Decline in Arctic sea ice thickness from submarine and ICESat records: 1958-2008, Geophys. Res. Lett., 36, L15501, doi:10.1029/2009GL039035.

[5] Maslanik, J. A., C. Fowler, J. Stroeve, S. Drobot, J. Zwally, D. Yi, and W. Emery (2007), A younger, thinner Arctic ice cover: Increased potential for rapid, extensive sea ice loss, Geophys. Res. Lett., 34, L24501, doi:10.1029/2007GL032043.

[6] Maslanik, J. A., J. Stroeve, C. Fowler, and W. Emery (2011), Distribution and trends in Arctic sea ice age through spring 2011, Geophys. Res. Lett., 38, L13502, doi:10.1029/2011GL047735.

[7] Renner, A. H. H., S. Gerland, C. Haas, G. Spreen, J. Beckers, E. Hansen, M. Nicolaus, and H. Goodwin (2014). Evidence of Arctic sea ice thinning from direct observations, Geophysical Research Letters, Vol. 119, doi: 10.1002/2014GL060369.

[8] Ekeberg, O-C., K. Høyland, E. Hansen and M. Tschudi (2014), Reduction in the Number and Draft of Ridges in the Transpolar Drift in the Fram Strait during 2006-2011, In Proceedings of the 22nd IAHR International Symposium on Ice, doi:10.3850/978-981-09-0750-1_1226, pp. 574-581.

[9] Hansen, E., O-C. Ekeberg, S. Gerland, O. Pavlova, G. Spreen, and M. Tschudi (2014). Variability in categories of Arctic sea ice in Fram Strait. Journal of Geophysical Research – Oceans, vol. 119, doi:10.1002/2014JC010048.

[10] Spreen, G., S. Gerland, and E. Hansen (2014), Sea ice thickness changes in Fram Strait and the Arctic Basin during 1990-2013 from moored sonars with emphasize on sea ice minimum years 2007 and 2012, In Proceedings of the 22nd IAHR International Symposium on Ice.

[11] Vinje, T., N. Nordlund, and Å. Kvambekk (1998), Monitoring ice thickness in Fram Strait, J. Geophys. Res., Vol. 103, No. C5, pp. 10,437-10,449.

[12] Melling, H., P.A. Johnston, and D.A. Riedel (1995), Measurement of the draft and topography of sea ice by moored subsea sonar, Journal of Atmospheric and Oceanic Technology, 13(3), 589-602.

[13] Kwok, R., G. F. Cunningham, and S. S. Pang (2004), Fram Strait sea ice outflow, J. Geophys. Res., 109, C01009, doi:10.1029/2003JC001785.

[14] Vinje, T., and Ø . Finnekåsa (1986), The ice transport through Fram Strait, *Norsk Polarinstitutt Skrifter*, No. 186, Norwegian Polar Institute *Skrifter* Series.

[15] Fowler, C., and M. Tschudi, 2003, updated 2008. Polar Pathfinder Daily 25 km EASE-Grid Sea Ice Motion Vectors, 1987-2006. Boulder, Colorado USA: National Snow and Ice Data Center, NSIDC. Digital Media

[16] Girard-Ardhuin, F., et al., 2008. Sea ice drift in the central Arctic combining Quikscat and SSMI sea ice drift data. Users manual, version 3.0 April 2008, CERSAT Ifremer.